Virtual experiments of Czochralski growth of silicon using machine learning: Influence of processing parameters on interstitial oxygen concentration

Kentaro Kutsukake [a],[*], Yuta Nagai [b], Hironori Banba [b]

[a] Center for Advanced Intelligence Project, RIKEN, Nihonbashi, Chuo-ku, Tokyo 103-0027, Japan
[b] GlobalWafers Japan Co., Ltd., Seiro, Niigata 957-0197, Japan

ARTICLE INFO

ABSTRACT

For a process development, it is crucial to know the influence of each process parameter on the process result. However, it is difficult to gauge the influence by experimentally changing only one parameter value owing to constraints of the combination of the parameter values and experimental costs. Machine learning models can predict results that will be obtained under conditions that have not been considered for the experiment. Utilizing a virtual experiment based on a machine learning model, we evaluated the influence of process parameters on the interstitial oxygen (Oi) concentration in Czochralski-grown Si crystals. A dataset for the parameter analysis was constructed, wherein the crucible rotation rate and/or Ar flow rate were systematically changed while maintaining the other parameters at the reference value of an experimental datum. Thereafter, the dataset was input into a neural network model that had been trained with 450 ingot data; consequently, the corresponding Oi concentration was obtained. The evaluated results were consistent with the scientific knowledge previously studied: Oi concentration increases with increasing crucible rotation rate and decreasing Ar flow rate. Furthermore, the two-parameter analysis illustrated a nonlinear relationship between the parameters quantitatively. These approaches demonstrating the Czochralski growth of Si in this study are useful in other crystal growth processes as well.

1. Introduction

Silicon (Si) crystals grown by the Czochralski (CZ) method are one of the most important semiconductor materials. Si crystals are used in wafers for semiconductor devices, such as integrated circuit chips and image sensors that comprise the foundation of a highly sophisticated information society. Si crystals are also important in carbon neutrals as substrate materials for energy conversion and energy generation, for example, in power devices and solar cells.

Oxygen is an important impurity in Si crystals; it influences the electrical properties and mechanical strength of wafers. In addition, oxygen precipitates that are formed during the cooling and annealing processes, function as gettering sites for metallic impurities. Thus, controlling the oxygen impurity concentration is crucial for the practical use of Si crystals [1–5].

The oxygen impurity concentration in Si ingots depends on the crystal growth conditions, as shown in Fig. 1 [6–8]. In the CZ Si crystal growth, the Si melt is contained in a silica (quartz) crucible. During the growth process, oxygen dissolves in the melt from the inner walls of the crucible and is transported inside the melt by diffusion and convection [9–13]. Although most of the oxygen evaporates from the surface of the melt as SiO gas, some oxygen is incorporated into the Si crystal. This extremely complicated incorporation process of oxygen is affected by process parameters, not only the parameters that directly influence the melt convections such as heater powers, crucible rotation rate, and magnetic field, but also the parameters that influence the gas convection, such as the Ar flow rate and pressure, and the parameters that influence the temperature field, such as the age of the graphite parts, and the condition of the inner wall of the growth chambers have an impact on the oxygen concentration. It is crucial to reveal the influence of the process parameters individually to precisely control the oxygen concentration. However, it is almost impossible to change only one parameter while keeping the other parameters constant in practical experiments.
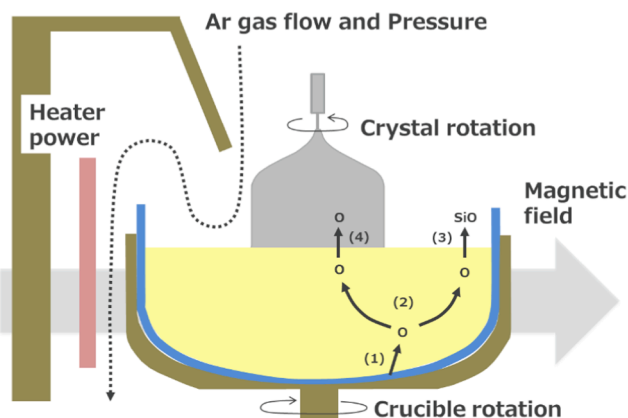
Fig. 1. Schematic illustration of incorporation process of oxygen into Si crystal. Oxygen is (1) dissolved from a silica crucible, (2) transported into the Si melt, (3) evaporated from the melt surface and (4) incorporated into the crystal. Many process parameters influence this incorporation process complexly.

Computational simulations provide an analysis of the oxygen incorporation. Based on the physical and chemical system of the crystal growth furnace, two-dimensional and three-dimensional numerical models of oxygen transport during crystal growth were developed to analyze the influence of process parameters on the oxygen concentration [14–19]. Brown et al. qualitatively calculated the interstitial oxygen (Oi) concentration in a crystal by analyzing the heat transfer and gas flow in a CZ furnace [20–22]. Togawa et al. reported a numerical analysis to investigate the impact of the crucible rotation rate, an essential parameter that controls the melt convection and Oi concentration in CZ Si crystals [23,24].

However, computational simulations have two issues in the practical application of CZ Si crystals. Although the calculation time decreases with the development of simulation techniques and computer performance, the computational cost is still high. In particular, in the case of parameter analysis, in which repeat simulation is necessary, the computational cost becomes significant. Another issue is the difference between the simulation and the actual results. Highly precise reproduction of the real result requires highly precise boundary conditions and physical property values, in addition to the precise physical model. For example, the inhomogeneity of the radiation factor of the inner wall of the growth chamber due to the precipitation of evaporated oxygen should be incorporated into the simulation as the boundary conditions for highly precise evaluations. However, it is almost impossible to measure and model such complicated inhomogeneity.

Recently, machine learning applications for material processes have attracted considerable attention. Machine learning allows us to predict the results under any parameter value conditions within the training data range in a significantly small computational duration when the model is trained appropriately. For crystal growth research, parameter analysis based on simulation results [25–27], optimization of process parameters using simulation data [28–32] and experimental data [33–35], have been reported.

In our previous study regarding CZ Si growth, we developed a machine learning model to predict the Oi concentration using the practical experimental data of 450 ingots. Utilizing the fast prediction of the experimental results using the machine learning model, we developed a real-time prediction system [36].

In this study, using the machine learning model developed in the previous study [36], we analyzed the influence of the process parameters on the Oi concentration. Because the machine learning mode was trained using the actual experimental result, we can solve the issues of the computational simulations mentioned above. In the analysis, only one process parameter was changed, while maintaining the other parameters constant. This corresponds to the virtual experiments of CZ growth. Among the parameters, the results of the crucible rotation rate and Ar flow rate are presented and discussed in comparison with the previously reported results.

2. Experiments

2.1. Experimental data and machine learning model

For machine learning, experimental data of 450 CZ crystal ingots grown in the same furnace in the presence of a magnetic field were used. The crystal diameter was 300 mm. The Oi concentration range of the samples was between 0.7×10^{18} atoms/cm^3 and 1.7×10^{18} atoms/cm^3, and the resistivity range was between 1.5 Ω·cm and 78.1 Ω·cm. The Oi concentration was measured via Fourier transform infrared spectroscopy (FT-IR) at several positions of each ingot. Three types of experimental data were used as input parameters for the machine learning model: fixed parameters such as the age of the graphite heater and crucible, process parameters such as ingot pulling rate, crucible rotation rate, and crystal rotation rate, and monitored parameters such as temperature and ingot diameter. The process parameters are controllable and set by the operator, and the monitored parameters are only for observation and are not directly controlled. The fixed parameters are fixed in a growth process and vary with the ingots. The addition of the monitored and fixed parameters to the input dataset that incorporates more information regarding the furnace condition, significantly improved the performance of the machine learning model. The total number of input parameters was 43. Merging these data with the Oi concentration value, we prepared a dataset for machine learning. The net data rows were 2209, and separated into 1554 training data and 655 test data. In particular, each ingot datum was assigned to one of these data groups to prevent data contamination. Finally, the parameter values were standardized using the standardization formula: $x' = (x-u)/\sigma$, where x' and x are the standardized and original parameter values, and u and σ are the mean and standard deviation of the parameter values of the training dataset, respectively.

The fully connected feedforward neural network model was constructed and trained using the Keras [37] and Tensorflow [38] libraries in Python. The number of layers, nodes in each layer, and epochs were 5, 128, and 20,000, respectively. Dropout and batch normalization were performed after every fully connected layer. A sigmoid activation function was applied, and the loss was measured using the mean squared error with a layer weight regularizer. The root mean squared error and R^2 score for the test data were 4.2×10^{16} atoms/cm^3 and 0.94, respectively. This prediction error is sufficiently low for the practical estimation and control of the Oi concentration. Details of the data structure of the experimental data, machine learning model, and the influence of the addition of monitored and fixed parameters on the machine learning accuracy are described in Ref. [36].

2.2. Data structure and evaluation procedure for parameter influences

Fig. 2 shows the procedure used to evaluate the influence of the parameters on the Oi concentration using the machine learning model. First, we selected one data row for the experimental conditions from the dataset. This condition served as a reference point for evaluation. Thereafter, the data rows were stacked above and below the experimental condition row, only changing the evaluation parameter value while maintaining the values in the other columns (Fig. 2 (a)). The evaluation parameter value was continuously changed in the range of -0.5σ to $+0.5\sigma$ around the experimental value, where σ is the standard deviation of the evaluation parameter in the training dataset. To evaluate the influence of two parameters, a combination of the two values on the mesh grid of the evaluation parameters was prepared, and the data rows were stacked as in the case of a single parameter.

Second, each data row was fed into the neural network model, and the corresponding Oi concentration was predicted, as shown in Fig. 2
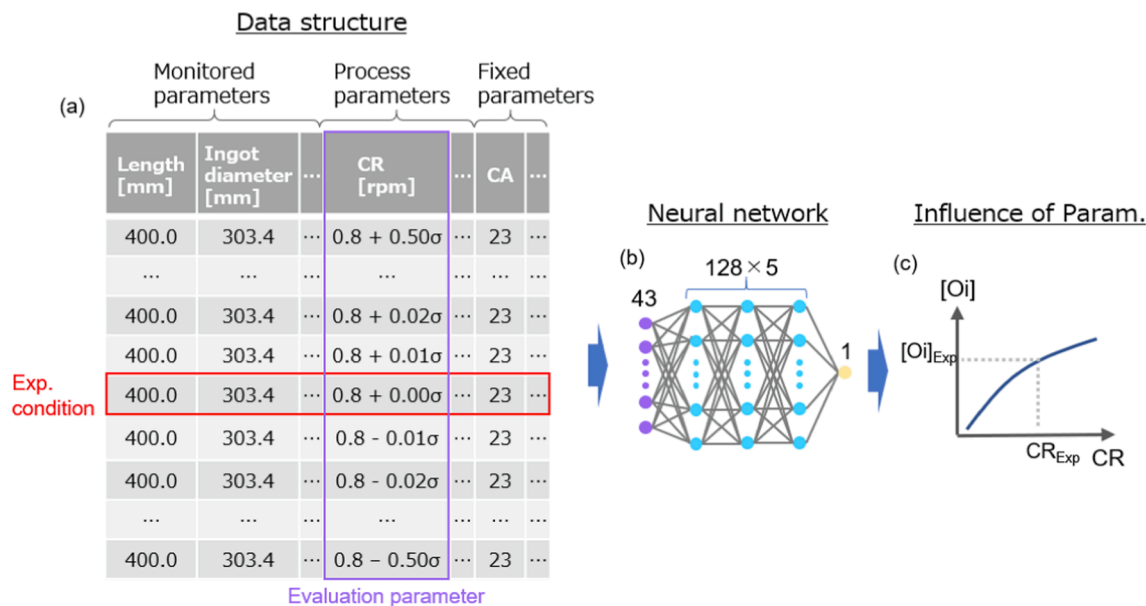
Fig. 2. Schematic illustration of the procedure to evaluate the influence of the parameters on Oi concentration using the machine learning model. (a) Data structure of the dataset for evaluation. CR is crucible rotation speed and the evaluation parameter in this example. CA is the crucible age. The values in the table are an example of the reference condition. (b) Neural network model. (c) Output image of this evaluation procedure. Experimental value of CR (CR_{Exp}) and Oi ($[Oi]_{Exp}$) are reference values for this evaluation.

(b). By applying this procedure to all the rows of the dataset for evaluation, a continuous change in Oi concentration with evaluation parameter change was obtained (Fig. 2 (c)).

3. Results and discussion

We selected three reference points with high (labeled A), middle (labeled B), and low (labeled C) Oi concentrations from the experimental dataset with ingot lengths between 400 mm and 600 mm. The influences of the crucible rotation rate and Ar flow rate were evaluated. Fig. 3 shows the change in Oi concentration around the reference points A, B, and C, when the evaluation parameter values changed from the reference conditions. The Oi concentration increased with an increase in the crucible rotation rate. This result is consistent with previous findings regarding the fact that oxygen dissolution from the quartz crucible increases with an increase in the crucible rotation rate [23,24]. Further, the Oi concentration decreases with increasing Ar gas flow rate. This result is also consistent with previous findings regarding the gas flow promoting SiO evaporation from the Si melt surface, resulting in a decrease in the oxygen concentration in the melt when the inward convection from the crucible wall is dominant [20–22].

As demonstrated above, the influence of the crucible rotation rate and Ar flow rate predicted by the machine learning model is consistent with the scientific explanations in the previous studies qualitatively. Furthermore, the machine learning model provides a nonlinear influence, depending on the other conditions quantitatively. For example, the dependence of the Oi concentration on the crucible rotation rate is logarithmic-like in reference condition A; in contrast, it is exponential-like around reference condition B. The decrease in Oi concentration by changing the Ar flow rate was large in reference condition C, while it had almost no influence around the reference condition A. These quantitative predictions around the actual experimental conditions facilitate controlling the Oi concentration more precisely.

Utilizing fast prediction through a machine learning model, we evaluated the Oi concentration distribution around the reference condition C as a function of the crucible rotation rate and Ar flow rate. The results are shown in Fig. 4. The complicated non-linear relationship between the parameters was successfully modeled as the prediction surface in the three-dimensional parameter space. For example, the slope of the Oi concentration change with the crucible rotation rate at a -0.5 Ar flow rate is steeper than that at a 0.5 Ar flow rate.

In this visualization, a total concentration of $100 \times 100 = 10000$ Oi is calculated that is impossible in conventional simulations because of the high computational cost. The calculation time of the machine learning model for all data was less than 1 s. This is an advantage of machine learning.

It should be noted that these analyses are virtual experiments. As mentioned in the experimental section, only one or two evaluation parameter values were changed while maintaining the other parameters at the values of the reference condition. This procedure can individually evaluate the influence of the evaluation parameters. In contrast, in real experiments using an actual furnace, the changes in the monitored parameters follow the changes in the process parameters during ingot growth. In other words, the monitored parameters depend on both the process parameter values and furnace conditions. Thus, to predict the actual influence of the process parameters, a simultaneous process parameter change should be considered. This is currently under study.

4. Summary

The influence of the process parameters on Oi concentration in the CZ Si crystals was analyzed using a machine learning model trained with the experimental data of 450 ingots. A data set for the analysis was developed by changing one parameter value while maintaining the other parameter values at the values of one experimental result. By inputting this dataset into the trained neural network model, the change in Oi concentration from the experimental value was estimated as a function of the changing parameter. Among the process parameters, the influences of the crucible rotation rate and Ar flow rate were analyzed. The Oi concentration increased with increasing crucible rotation rate and decreasing Ar flow rate. These tendencies are consistent with previously reported scientific knowledge. Furthermore, the nonlinear interaction between the influence of the two parameters was quantitatively visualized as a two-dimensional surface in the parameter space. The applications of the machine learning model demonstrated in this study will be useful not only for CZ Si growth, but also for other crystal
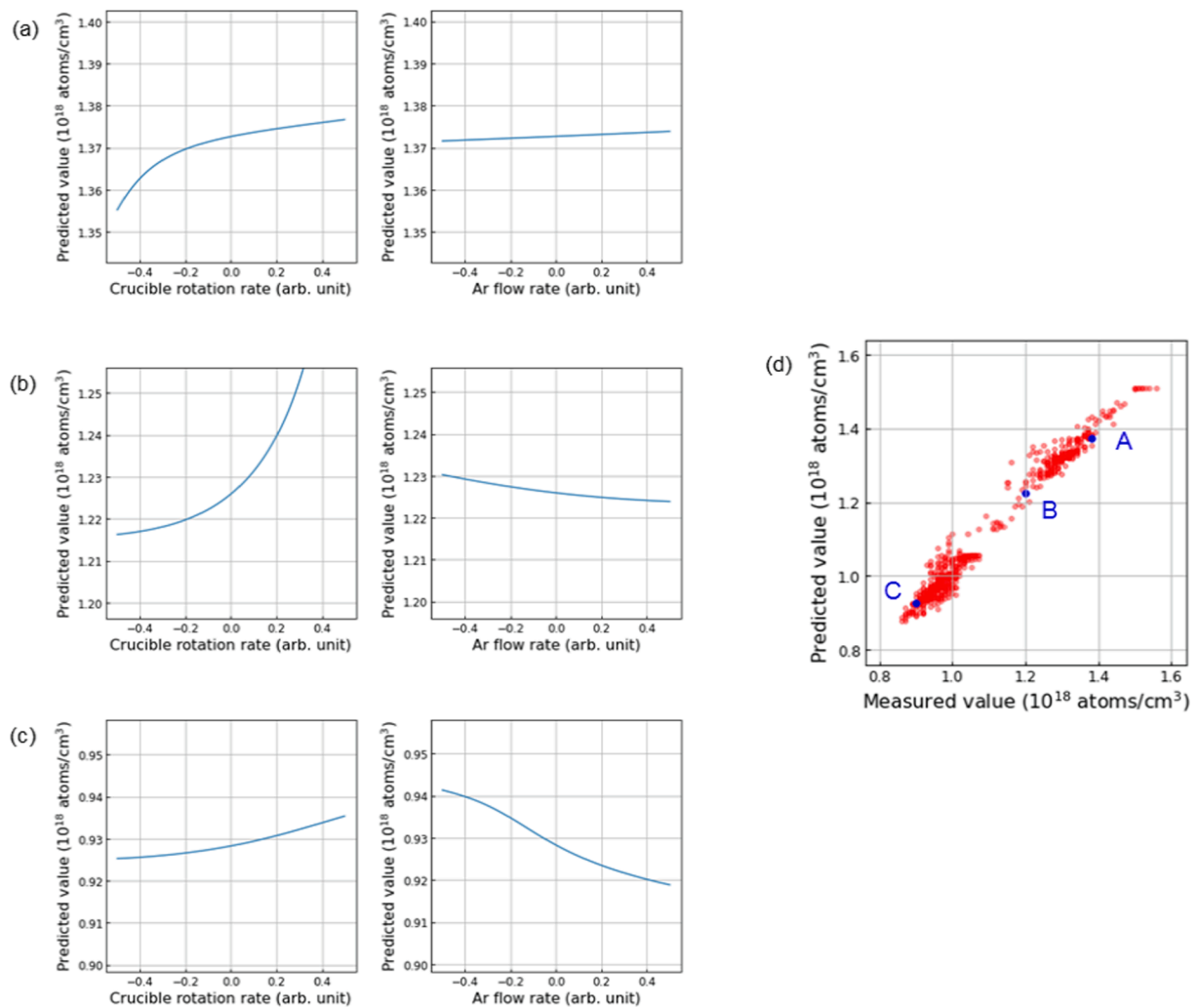
Fig. 3. Influence of crucible rotation rate and Ar flow rate on Oi concentration. (a), (b), and (c) represent the evaluation results around the reference points with high, middle, and low Oi concentration shown as A, B, and C in Fig. 3(d). The value range of the vertical axes was set at the same scale. The zero position of the horizontal axes corresponds to the value of the reference condition. (d) Relationship between measured and predicted values of Oi concentration for the test dataset.
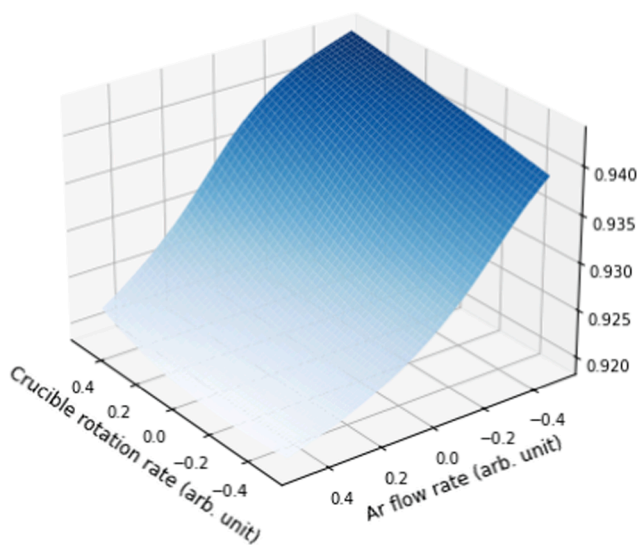

Fig. 4. Prediction surface of Oi concentration around the reference point C as functions of crucible rotation rate and Ar flow rate.

growth processes, including thin growth from vaper, and material processes, such as slicing, grinding, and polishing.

Funding

CRediT authorship contribution statement

Kentaro Kutsukake: Conceptualization, Methodology, Software, Investigation, Writing – original draft. **Yuta Nagai:** Investigation, Validation, Writing – review & editing, Project administration. **Hironori Banba:** Investigation, Validation, Data curation.

Declaration of Competing Interest

The authors declare that they have no known competing financial interests or personal relationships that could have appeared to influence the work reported in this paper.

Acknowledgments

References

[1] S. Kishino, Y. Matsushita, M. Kanamori, T. Iizuka, Thermally induced microdefects in Czochralski-Grown silicon: Nucleation and growth behavior, Jpn. J. Appl. Phys. 21 (Part 1, No. 1) (1982) 1–12, https://doi.org/10.1143/JJAP.21.1.

[2] K. Hoshikawa, H. Kohda, K. Ikuta, Improvement in CZ silicon wafer by reducing oxygen impurity, Jpn. J. Appl. Phys. 20 (S1) (1981) 241, https://doi.org/10.7567/JJAPS.20S1.241.

[3] S.M. Hu, W.J. Patrick, Effect of oxygen on dislocation movement in silicon, J. Appl. Phys. 46 (5) (1975) 1869–1874, https://doi.org/10.1063/1.321883.

[4] K. Sumino, H. Harada, I. Yonenaga, The origin of the difference in the mechanical strengths of Czochralski-grown silicon and float-zone-grown silicon, Jpn. J. Appl. Phys. 19 (1) (1980) L49–L52, https://doi.org/10.1143/JJAP.19.L49.

[5] T.Y. Tan, E.E. Gardner, W.K. Tice, Intrinsic gettering by oxide precipitate induced dislocations in Czochralski Si, Appl. Phys. Lett. 30 (4) (1977) 175–176, https://doi.org/10.1063/1.89340.

[6] K. Hoshikawa, H. Hirata, H. Nakanishi, K. Ikuta, in: Semiconductor Silicon, The Electrochemical Society, Pennington, New Jersey, 1981, p. 101.

[7] A. Murgai, in: Semiconductor Silicon, The Electrochemical Society, Pennington, New Jersey, 1981, p. 113.

[8] T. Carlberg, T.B. King, A.F. Witt, Dynamic oxygen equilibrium in silicon melts during crystal growth by the Czochralski technique, J. Electrochem. Soc. 129 (1) (1982) 189–193, https://doi.org/10.1149/1.2123753.

[9] H. Hirata, K. Hoshikawa, The dissolution rate of silica in molten silicon, Jpn. J. Appl. Phys. 19 (8) (1980) 1573–1574, https://doi.org/10.1143/JJAP.19.1573.

[10] R.E. Chaney, C.J. Varker, The dissolution of fused silica in molten silicon, J. Cryst. Growth. 33 (1) (1976) 188–190, https://doi.org/10.1016/0022-0248(76)90101-9.

[11] K. Abe, K. Terashima, T. Matsumoto, S. Maeda, H. Nakanishi, Fused quartz dissolution rate in silicon melts: influence of boron addition, J. Cryst. Growth. 186 (4) (1998) 557–564, https://doi.org/10.1016/S0022-0248(97)00618-0.

[12] X. Huang, K. Saitou, S. Sakai, K. Terashima, K. Hoshikawa, Analysis of oxygen evaporation rate and dissolution rate concerning Czochralski Si crystal growth: effect of Ar pressure, Jpn. J. Appl. Phys. 37 (Part 1, No. 6A) (1998) 3188–3193, https://doi.org/10.1143/JJAP.37.3188.

[13] X. Huang, K. Saitou, S. Sakai, K. Terashima, K. Hoshikawa, Analysis of an oxygen dissolution process concerning Czochralski (CZ) Si crystal growth using the sessile drop method, Jpn. J. Appl. Phys. 37 (Part 2, No. 2B) (1998) L193–L195, https://doi.org/10.1143/JJAP.37.L193.

[14] K. Kakimoto, K.-W. Yi, M. Eguchi, Oxygen transfer during single silicon crystal growth in Czochralski system with vertical magnetic fields, J. Cryst. Growth. 163 (3) (1996) 238–242, https://doi.org/10.1016/0022-0248(95)00976-0.

[15] K. Kakimoto, M. Eguchi, H. Ozoe, Use of an inhomogenous magnetic field for silicon crystal growth, J. Cryst. Growth. 180 (3-4) (1997) 442–449, https://doi.org/10.1016/S0022-0248(97)00239-X.

[16] L. Liu, K. Kakimoto, Partly three-dimensional global modeling of a silicon Czochralski furnace. II. Model application: analysis of a silicon Czochralski furnace in a transverse magnetic field, Int. J. Heat Mass Transf. 48 (21-22) (2005) 4492–4497, https://doi.org/10.1016/j.ijheatmasstransfer.2005.04.030.

[17] A.D. Smirnov, V.V. Kalaev, Development of oxygen transport model in Czochralski growth of silicon crystals, J. Cryst. Growth. 310 (12) (2008) 2970–2976, https://doi.org/10.1016/j.jcrysgro.2008.03.002.

[18] B. Gao, K. Kakimoto, Global simulation of coupled carbon and oxygen transport in a Czochralski furnace for silicon crystal growth, J. Cryst. Growth. 312 (20) (2010) 2972–2976, https://doi.org/10.1016/j.jcrysgro.2010.07.026.

[19] B. Gao, S. Nakano, K. Kakimoto, Global simulation of coupled carbon and oxygen transport in a unidirectional solidification furnace for solar cells, J. Electrochem. Soc. 157 (2) (2010) H153, https://doi.org/10.1149/1.3262584.

[20] R.A. Brown, T.A. Kinney, P.A. Sackinger, D.E. Bornside, Toward an integrated analysis of czochralski growth, J. Cryst. Growth. 97 (1) (1989) 99–115, https://doi.org/10.1016/0022-0248(89)90252-2.

[21] T.K. Kinney, D.E. Bornside, W. Zhou, R.A. Brown, in: Semiconductor Silicon, The Electrochemical Society, Pennington, New Jersey, 1994, p. 90.

[22] D.E. Bornside, R.A. Brown, T. Fujiwara, H. Fujiwara, T. Kubo, The effects of gas-phase convection on carbon contamination of Czochralski-Grown silicon, J. Electrochem. Soc. 142 (8) (1995) 2790–2804, https://doi.org/10.1149/1.2050094.

[23] S. Togawa, Y. Shiraishi, K. Terashima, S. Kimura, Oxygen transport mechanism in Czochralski silicon melt: I. The Whole Bulk Melt, J. Electrochem. Soc. 142 (8) (1995) 2839–2844, https://doi.org/10.1149/1.2050102.

[24] S. Togawa, Y. Shiraishi, K. Terashima, S. Kimura, Oxygen transport mechanism in Czochralski silicon melt: II Vicinity of growth interface, J. Electrochem. Soc. 142 (8) (1995) 2844–2848, https://doi.org/10.1149/1.2050103.

[25] N. Dropka, M. Holena, Optimization of magnetically driven directional solidification of silicon using artificial neural networks and Gaussian process models, J. Cryst. Growth. 471 (2017) 53–61, https://doi.org/10.1016/j.jcrysgro.2017.05.007.

[26] Y. Tsunooka, N. Kokubo, G. Hatasa, S. Harada, M. Tagawa, T. Ujihara, High-speed prediction of computational fluid dynamics simulation in crystal growth, Cryst, Eng. Commun 20 (41) (2018) 6546–6550, https://doi.org/10.1039/C8CE00977E.

[27] A. Boucetta, K. Kutsukake, T. Kojima, H. Kudo, T. Matsumoto, N. Usami, Application of artificial neural network to optimize sensor positions for accurate monitoring: an example with thermocouples in a crystal growth furnace, Appl. Phys. Express. 12 (12) (2019) 125503, https://doi.org/10.7567/1882-0786/ab52a9.

[28] Y. Takehara, A. Sekimoto, Y. Okano, T. Ujihara, S. Dost, Bayesian optimization for a high- and uniform-crystal growth rate in the top-seeded solution growth process of silicon carbide under applied magnetic field and seed rotation, J. Cryst. Growth. 532 (2020) 125437, https://doi.org/10.1016/j.jcrysgro.2019.125437.

[29] Y. Dang, L. Liu, Z. Li, Optimization of the controlling recipe in quasi-single crystalline silicon growth using artificial neural network and genetic algorithm, J. Cryst. Growth. 522 (2019) 195–203, https://doi.org/10.1016/j.jcrysgro.2019.06.033.

[30] K. Matsui, S. Kusakawa, K. Ando, K. Kutsukake, T. Ujihara, I. Takeuchi, preprint arXiv:1911.03671 [math-ph] (2019).

[31] W. Yu, C. Zhu, Y. Tsunooka, W. Huang, Y. Dang, K. Kutsukake, S. Harada, M. Tagawa, T. Ujihara, Geometrical design of a crystal growth system guided by a machine learning algorithm, CrystEngComm 23 (14) (2021) 2695–2702, https://doi.org/10.1039/D1CE00106J.

[32] Y. Dang, C. Zhu, M. Ikumi, M. Takaishi, W. Yu, W. Huang, X. Liu, K. Kutsukake, S. Harada, M. Tagawa, T. Ujihara, Adaptive process control for crystal growth using machine learning for high-speed prediction: application to SiC solution growth, CrystEngComm. 23 (9) (2021) 1982–1990, https://doi.org/10.1039/D0CE01824D.

[33] K. Osada, K. Kutsukake, J. Yamamoto, S. Yamashita, T. Kodera, Y. Nagai, T. Horikawa, K. Matsui, I. Takeuchi, T. Ujihara, Adaptive Bayesian optimization for epitaxial growth of Si thin films under various constraints, Mater. Today Commun. 25 (2020) 101538, https://doi.org/10.1016/j.mtcomm.2020.101538.

[34] S. Miyagawa, K. Gotoh, K. Kutsukake, Y. Kurokawa, N. Usami, Application of Bayesian optimization for improved passivation performance in TiOx/SiOy/c-Si heterostructure by hydrogen plasma treatment, Appl. Phys. Express. 14–2 (2021), 025503. https://doi.org/10.35848/1882-0786/abd869.

[35] S. Miyagawa, K. Gotoh, K. Kutsukake, Y. Kurokawa, N. Usami, Application of Bayesian optimization for high-performance TiO /SiO /c-Si passivating contact, Sol. Energy Mater. Sol. Cells. 230 (2021) 111251, https://doi.org/10.1016/j.solmat.2021.111251.

[36] K. Kutsukake, Y. Nagai, T. Horikawa, H. Banba, Real-time prediction of interstitial oxygen concentration in Czochralski silicon using machine learning, Appl. Phys. Express. 13 (2020), 125502. https://doi.org/10.35848/1882-0786/abc6ec.

[37] Keras. https://keras.io. (accessed 26 October 2021).

[38] TensorFlow, Large-scale machine learning on heterogeneous systems, Software, 2015. tensorflow.org. (accessed 26 October 2021).